Journal of Petroleum Science and Engineering 182 (2019) 106270

Contents lists available at ScienceDirect

Journal of Petroleum Science and Engineering

journal homepage: www.elsevier.com/locate/petrol

Prediction of natural gas hydrates formation using a combination of thermodynamic and neural network modeling

Noura Rebai[a,b], Ahmed Hadjadj[a], Abdelbaki Benmounah[a], Abdallah S. Berrouk[c,*], Salim M. Boualleg[b]

[a] Unité de Recherche Matériaux - Procédés et Environnement (UR-MPE), Faculté des Sciences de l'Ingénieur, Université M'Hamed BOUGARA de Boumerdes, Avenue de l'indépendance, 35000, Boumerdes, Algeria
[b] Algerian Petroleum Institute, Boumerdes, 35000, Algeria
[c] Mechanical Engineering Department, Khalifa University of Science and Technology, Petroleum Institute, P.O. Box 2533, Abu Dhabi, United Arab Emirates

ARTICLE INFO

Keywords:
Gas hydrate formation
Van der Waals-Platteeuw models
Artificial neural network
Backpropagation algorithm

ABSTRACT

During the treatment or transport of natural gas, the presence of water, even in very small quantities, can trigger hydrates formation that causes plugging of gas lines and cryogenic exchangers and even irreversible damages to expansion valves, turbo expanders and other key equipment. Hence, the need for a timely control and monitoring of gas hydrate formation conditions is crucial.

This work presents a two-legged approach that combines thermodynamics and artificial neural network modeling to enhance the accuracy with which hydrates formation conditions are predicted particularly for gas mixture systems. For the latter, Van der Waals-Platteeuw thermodynamic model proves very inaccurate. To improve the accuracy of its predictions, an additional corrective term has been approximated using a trained network of artificial neurons. The validation of this approach using a database of 4660 data points shows a significant decrease in the overall relative error on the pressure from around 23.75%–3.15%. The approach can be extended for more complicated systems and for the prediction of other thermodynamics properties related to the formation of hydrates.

1. Introduction

Gas hydrates are nonstoichiometric crystalline, ice-like mixtures, consisting of a frame of water cages occupied by gas molecules such as methane, ethane and CO_2. In the oil and gas transportation systems, the presence and accumulation of gas hydrates under high pressure and low temperature conditions can eventually form solid particles. The latter could partially plug or completely block pipelines and may lead to severe equipment and environmental damage and to fatal injuries (Gbaruko et al., 2007; Mooijer–van den Heuvel, 2004). Preventing the formation of gas hydrates by injecting thermodynamic inhibitors (such as methanol and ethylene glycol) to shift the hydrate formation temperature to a lower zone in the pipeline is the most widely used method for field operation in the oil and gas industry (Lederhos, 1996; Lachet and Béhar, 2000). However, the costs related to this thermodynamic injection method is unattractive and the recovery of the inhibitors is often difficult and environmentally unfriendly. It was estimated that the cost born by offshore oil and gas transport operations for hydrate prevention can be as high as approximately one million dollars per mile (Jassim et al., 2008; John et al., 1985Gudmundsson and Børrehaug, 1996). For these reasons, prediction of hydrate formation conditions has become a major interest for the gas industry, and the subject of abundant research (Lachet and Béhar, 2000, Gudmundsson and Børrehaug, 1996). X-ray analysis of the hydrates crystals has made it possible to identify three types of hydrates structures (sI, sII and sH), within which natural gas molecules are able to form the first two structures (Sloan, 1998). In the literature, several works using thermodynamic modeling (Fouad and Berrouk, 2012, 2013), modification of mixing rules and approximation of interaction coefficients between molecules for predicting hydrates formation are proposed (Sloan, 1998; Sloan, 1990; Ballard, 2002; Berecz and Bella-achs, 1983; Holder et al., 1988).

Artificial intelligence techniques such as Artificial Neural Network (ANN), Support Vector Machine (SVM, LSSVM) and Extremely Randomized Trees are considered eligible to reproduce any form of a function, performing a matching of two spaces, if sufficient examples representing the behavior of this function are provided. In fact, those methods have been used successfully in the prediction of several

* Corresponding author.
E-mail address: abdallah.berrouk@ku.ac.ae (A.S. Berrouk).

https://doi.org/10.1016/j.petrol.2019.106270
Received 16 March 2019; Received in revised form 12 July 2019; Accepted 13 July 2019
Available online 15 July 2019
0920-4105/

thermodynamic parameters like freezing point depression of electrolyte solutions (Hamidreza et al., 2014), minimum initial temperature of a natural gas passing through a JT expansion without the risk of hydrate formation (Hamidreza et al., 2018), and component solubility (Helei et al., 2019).

The pioneer work on the use of ANN to enhance the prediction of hydrate formation conditions dates back to 1998 when Elgibaly and Elkamel (1998) obtained an average error of about 19% using a dataset of 2389 points. Chapoy et al., 2007 developed a neural network for the calculation of natural gas hydrate formation conditions in the presence and absence of inhibitors in the aqueous phase. They collected 3296 data points to be used for the ANN model's learning and validation. In order to predict the hydrate formation conditions of the binary hydrocarbon mixtures (CH4 + C2H6, CH4 + C3H8, CH4 + I-C4H10, CH4 + N-C4H10), Moradi, et al., 2013 used a dataset of 250 experimental points of which 70% for the learning phase and the rest for the validation phase. Their results show a good consistency with the experimental data. Mohammadi and Richon (2010a, b) demonstrated the ability of ANN models to determine hydrate formation conditions of hydrogen and methane in the presence of hydrate promoters such as tetrahydrofuran and tert-butylamine. The latter are used to reduce the pressure of hydrate formation. Their ANN models suffered a small deviation from the experimental data compared to the predictions of the thermodynamic models tested for the same mixtures (Mohammadi and Richon, 2010a, b). Babakhani et al., 2015 Optimized an ANN model used to predict the hydrate formation conditions of binary mixtures based on experimental data composed of 895 points. A relative error of 1.02% was recorded while a better prediction was obtained when compared to Colorado School of Mines Hydrate (CSMHYD) program's results. Hydrates formation conditions for more complicated systems were predicted using ANN such as tetrahydrofuran + methane, carbon dioxide or nitrogen (Mohammadi and Martinez-lopez, 2010), hydrogen + tetra-n-butyl ammonium bromide + water (Mohammadi et al., 2010).

ANN technique was also used for systems containing acid gases such as CO2 and very satisfactory results were obtained (Nezhad and Aminian, 2012; Ghavipour et al., 2013, and Babakhani et al., 2015). More recently, Hamidreza and Mohammad, 2017 proposed the use of two new approaches: “Extremely randomizes trees” and “LSSVM” to predict hydrate formation temperature. A database of 1800 experimental points was used for training and testing the model. The test of those methods on 10% of the data shows an average relative error, on the temperature prediction, of 0.04% and 0.32% respectively.

In this work, we present a two-legged approach that combines thermodynamics and artificial neural network modeling to enhance the accuracy with which hydrates formation conditions are predicted. The purpose is to improve the poor accuracy with which Van der Waals-Platteeuw thermodynamic model predicts pressure of hydrate formation for gas mixture systems. The trained artificial neurons network is used to estimate an additional pressure corrective term using a database of 11403 data points (6743 points for training exercises and 4660 points for validation set).

2. Equilibrium conditions for gas hydates formation

It is possible to determine the conditions under which the first hydrate crystals appear in the liquid phase, the prevention of hydrates is then ensured by maintaining a higher temperature and/or a lower pressure with regard to these formation conditions. The condition of thermodynamic equilibrium Hydrate-Gas-Water is expressed as follows (Mooijer–van den Heuvel, 2004; Sloan, 1998; Ballard, 2002; Holder et al., 1988; Barkan and Sheinin, 1993):

$$\Delta\mu_w^H = \Delta\mu_w^{L/I} \tag{1}$$

with:

$$\Delta\mu_w^H = \mu_w^H - \mu_w^\beta \tag{2a}$$

and

$$\Delta\mu_w^{L/I} = \mu_w^{L/I} - \mu_w^\beta \tag{2b}$$

where:

μ_W^H: Chemical potential of water in hydrate phase (H).
$\mu_W^{L/I}$: Chemical potential of water in aqueous phase, liquid (L) or solid (I).
μ_W^β: Chemical potential of hypothetical phase water (reference state) consisting of gas-free hydrate (β).

The calculation of the equilibrium conditions of the three phases (Hydrate/Gas/Water) leads to the determination of conditions (T, p, x) which pairs with Equation (1). The expressions of the two chemical potential differences are presented in the following sections.

2.1. Hydrate phase

The calculation of the chemical potential of water in the hydrate phase is based on the *Van der Waals and Platteeuw* model (Mooijer–van den Heuvel, 2004; Sloan, 1990; Gudmundsson and Børrehaug, 1996; Ballard, 2002) which is derived from statistical thermodynamics, and based on an analogy to the classical adsorption theory:

$$\mu_w^H = \mu_w^\beta + RT\sum_i v_i ln\left(1 - \sum_j \theta_{ij}\right) \tag{3}$$

The possibility of occupying the cavity i by the molecule j, expressed by (θ_{ij}), is given by the following expression:

$$\theta_{ij} = \frac{C_{ij}.\, f_j}{1 + \sum_j C_{ij}.\, f_j} \tag{4}$$

Where:

v_i: Number of cavities of type i per water molecule in lattice
R: Perfect gases constant ($8.3144\, J/(mol{\cdot}K)$),
T: Temperature (K).

In equation (4), f_j represents the fugacity of the constituent j in the gaseous phase and C_{ij} is the Langmuir constant relative to the constituent j occupying the cavity of type i. The latter is given by the relation:

$$C_{ij} = \frac{4\pi}{kT}\int_0^{Rj-aj} \exp\frac{-\sum_n W_{ij}^{(n)}(r)}{kT}.\, r^2 dr \tag{5}$$

where

n: number of layers formed by water molecules surrounding the cavity i
W_{ij}: Kihara interaction potential which expresses the average interaction energy between the encaged molecule j and the water molecules forming the cavity i
R1: Radius of the first layer of the cavity i (m)

The potential of Kihara is defined by the following relation:

$$W(r) = 2Z\varepsilon\left[\frac{\sigma^{12}}{R^{11}r}\left(\delta^{10} + \frac{a}{R}\delta^{11}\right) - \frac{\sigma^6}{R^5 r}\left(\delta^4 + \frac{a}{R}\delta^5\right)\right] \tag{6}$$

Where:

$$\delta^N = [(1 - r/R - a/R)^{-N} - (1 + r/R - a/R)^{-N}]/N \tag{7}$$

Z: Coordinations number which designates the number of Oxygen atoms per cavity
δ: Function given by Equation (7) with N = 4, 5, 10, 11

ε: Maximum attraction energy that is often said Kihara energy parameter
σ: Kihara distance parameter
a: Radius of the solid nucleus of the encaged molecule
R: cell radius of the cavity.

Kihara parameters are usually adjusted using experimental data of hydrate formation conditions in order to have the difference between the chemical potential of water in the hydrate phase and that of water in the aqueous phase less than or equal to a certain imposed tolerance.

2.2. Aqueous phase

The chemical potential of water in the aqueous phase is given as a function of temperature and pressure by the expression developed by Holder et al., 1988 (Sloan, 1998; Sloan, 1990; Holder et al., 1988):

$$\frac{\Delta\mu_W}{RT} = \frac{\Delta\mu_w^0}{RT} - \int_{T_0}^{T} \frac{\Delta h_w}{RT^2} dT + \int_0^P \frac{\Delta V_w}{RT} dP - ln\,(a_w) \tag{8}$$

where:

$$\Delta h_w = \Delta h_w^0 + \int_{T_0}^{T} \Delta C_{pw} dT \tag{9}$$

and:

$$\Delta C_{pw} = \Delta C_{PW}^0 + \alpha(T - T_0) \tag{10}$$

The four main parameters of these equations are defined as follows:

$\Delta\mu_w^0$: The difference between the chemical potential of the water in the hypothetical phase and that of water in the aqueous phase (L/I) (calculated at T = 273.15 K and P = 0 atm);
Δh_w^0: The difference between the molar enthalpy of water in the hypothetical phase and that of water in the aqueous phase (L/I) (calculated at T = 273.15 K and P = 0 atm);
ΔV_w: Difference between the molar volumes of water in the two phases mentioned above;
a_w: Water activity.

The activity of the water depends on the amount of gas dissolved in the aqueous phase. It is expressed, in this case, by the fraction of the water present in this phase:

$$a_w = 1 - \sum_j^n x_j \tag{11}$$

Where n is the number of constituents dissolved in water and Xj shows the molar fraction of the constituent j in the liquid phase. The values of the parameters necessary for the calculation of the chemical potential are presented in Table 1 with T_0 = 273.15 K.

3. Thermodynamic modeling results

The monitoring of phase equilibrium for methane, ethane and propane are established using a Van der Waals and Platteeuw thermodynamic model. The evolution of hydrate formation pressure versus temperature of those components is illustrated in Figs. 1–3.

In order to test the effectiveness of the thermodynamic modeling of hydrate formation conditions, we calculate the deviation of the obtained results from the experimental data available in the literature (Berecz, and Bella-achs, 1983; Rouher and Barduhn, 1969; Selleck et al., 1952; Holder and Hand, 1982).

Pure gases CH4, C2H6, C3H8, N2, CO2, H2S, i-C4H10, n-C4H10 and some mixtures are considered in the performance evaluation of the developed model. For this purpose, the predicted pressures Average Relative Error (ARE) for different temperature ranges is calculated

Table 1
Properties of the reference state.

Parameter	Structure I	Structure II
$\Delta\mu_w^0$ (j/mol)	1297	975
Δh_w^0 (j/mol) $T \geq T_0$	−4316	−5226
$T < T_o$	1395	785
ΔV_w^0 (ml/mol) $T \geq T_0$	4.596	4.996
$T < T_o$	2.996	3.396
ΔC_{pw}^0(j/mol.K) $T \geq T_0$	−34.583	−36.8607
$T < T_o$	3.315	1.029
α (j/mol.K) $T \geq T_0$	0.1890	0.1809
$T < T_o$	0.0121	0.00377

* Mixture containing: N_2 0.42/CO_2 0.38/CH_4 45.59/C_2H_6 49.02/C_3H_8 4.53/i-C_4H_{10} 0.04/n-C_4H_{10} 0.02., ** Natural gas from În-Salah gas field: N_2 0.39/CO_2 3.64/CH_4 94.41/C_2H_6 1.42/C_3H_8 0.12/i-C_4H_{10} 0.01/n-C_4H_{10} 0.01., *** Natural gas from Hassi Messaoud/South oil field: N_2 2.3/CO_2 1.16/CH_4 51.63/C_2H_6 23.36/C_3H_8 15.61/i-C_4H_{10} 1.32/n-C_4H_{10} 3.71/C_5^+ 0.91.).

according to the following expression:

$$ARE = \frac{1}{N} \sum_N \left| \frac{P^{exp} - P^{cal}}{P^{exp}} \right| \tag{12}$$

With:

P^{exp}: Hydrate formation pressure experimentally obtained at a given temperature
P^{cal}: Hydrate formation pressure predicted at the same temperature
N: Number of experimental points

Table 2 presents the values of the average relative error determined for some systems.

The results obtained for 167 points of pure gases present an overall error of the order of 2.785% whereas for the 68 points of simple mixture of two or three components is approximately 2.695%. For both pure and binary gases, the average relative error is found to be low. In the case of gas mixture, the results obtained show a significant deviation from the experimental hydrate formation data. This deviation is justified by the existence of interactions between the gas molecules trapped in the different cavities, which is not accounted for in the Van der Waals and Platteeuw model. Similar conclusions have been also obtained by Barkan and Sheinin (1993); Chen and Guo (1996); Klauda and Snadler (2003) with a relative error as high as 40% for such systems.

4. Artificial neural network (ANN) model

In order to take into consideration the interactions between the different molecules in gas mixture systems, and thus improve the prediction of the hydrate formation conditions, an approach based on combining thermodynamic and Artificial Neural Network (ANN) models is proposed and its accuracy is validated against field data.

4.1. Principle of our contribution to the prediction of hydrate formation conditions

The approach consists of the following steps:

- The chemical potential of water in the hydrate phase is given by Van Der Waals and Platieeuw model.
- The chemical potential of the water in the aqueous phase is given by the expression of Holder et al., 1988.
- The phase equilibrium is expressed by equation (1). The solution of this equation, for a fixed temperature, gives the hydrate formation pressure (p).
- The non-ideality of the system and the interactions forces between

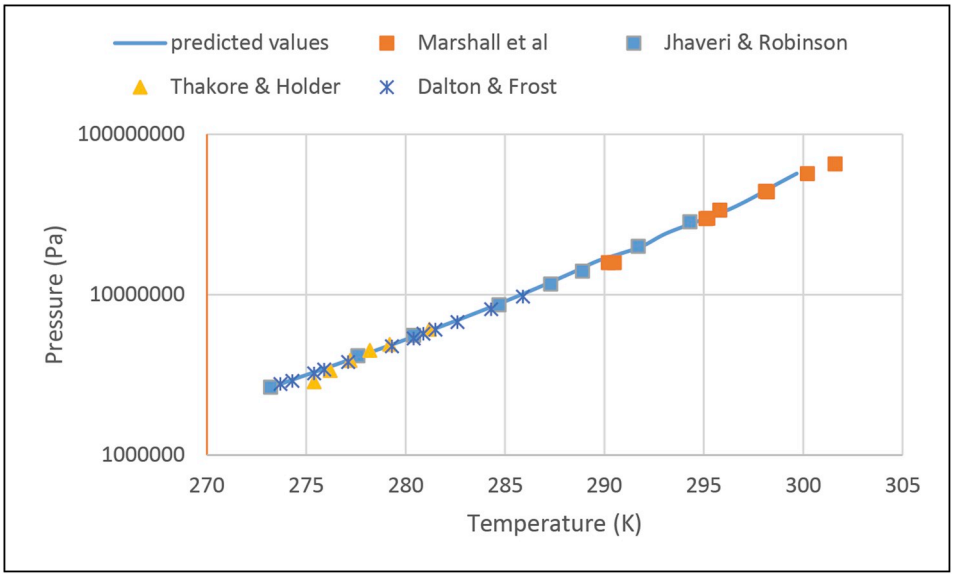

Fig. 1. Methane Hydrates pressure vs temperature.

the molecules encaged in the different cavities lead to the formation of hydrates at another pressure. $P_{new} = P + \boldsymbol{f}(P, T, y.....)$.

➢ ANN model is applied to determine the unknown function $\boldsymbol{f}$ bringing the value of P_{new} closer to the real value of the hydrate formation pressure ($P_{real} = P_{new}$).

Fig. 4 depicts the different steps of the two-legged approach used for the prediction of hydrates formation conditions of gas mixture systems.

The use of ANN model for the approximation of any function is possible as long as there is a sufficient number of data which characterises the inputs/outputs of the function to be approximated. The architecture, generally used to approximate a function, is the multilayer perceptron (Fausett, 1993; Ksabov, 1998). The Multi-Layer Perceptron (MLP) is a cascade of neurons where input vector communicates with all the neurons of the first layer.

The outputs of the neurons of this layer are then communicated to the neurons of the next layer, and so on. The last network layer is called the output layer while the others are referred to as hidden layers (Ksabov, 1998). Herein, MLP is used when the architecture has only one intermediate layer, the input vector is composed of temperature, thermodynamic pressure and composition of the gas. The composition of the natural gas may contain the following components: methane, ethane, propane, iso-butane, normal butane, nitrogen, carbon dioxide, hydrogen sulfide. Whereas the output vector has only one component, which is the pressure correction. The architecture proposed herein is illustrated in Fig. 5.

Any ANN model requires a learning phase, which aims to fix the weights of connections, w_{ij}, so that the network is able to perform a given transformation, represented by a set of examples consisting of a sequence of **K** input vectors associated with another sequence of desired output vectors. The calculation of the weights of a neural network can be simply formulated as an optimization problem which consists of finding a vector w which minimizes the quadratic error, E, on the basis of learning (Haykin, 2009).

Among the ANN learning algorithms that use gradient decent is backpropagation algorithm. The latter is one of the simplest and most efficient algorithms for hidden-cell networks. For a simple architecture with a single hidden layer and one output layer with a single cell, the

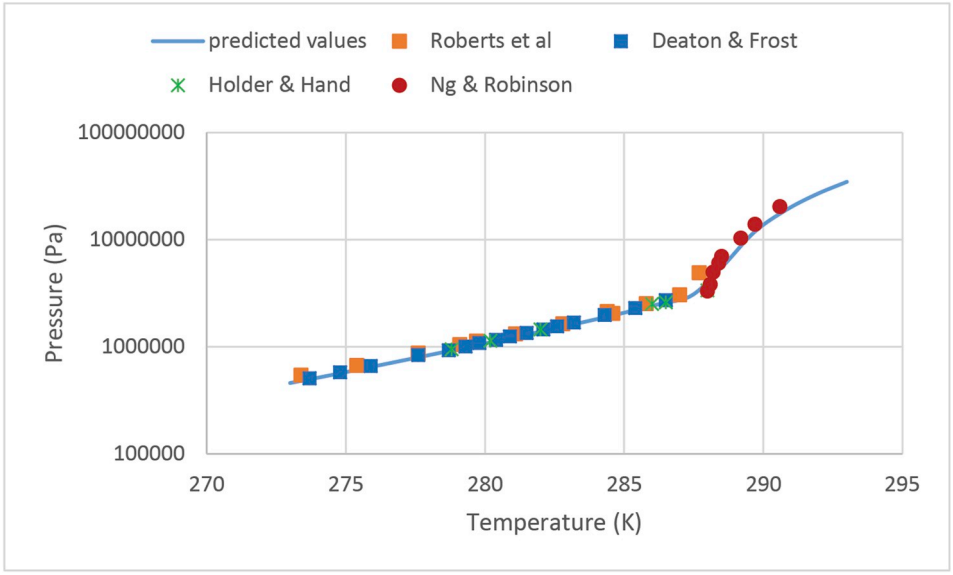

Fig. 2. Ethane Hydrates pressure vs temperature.

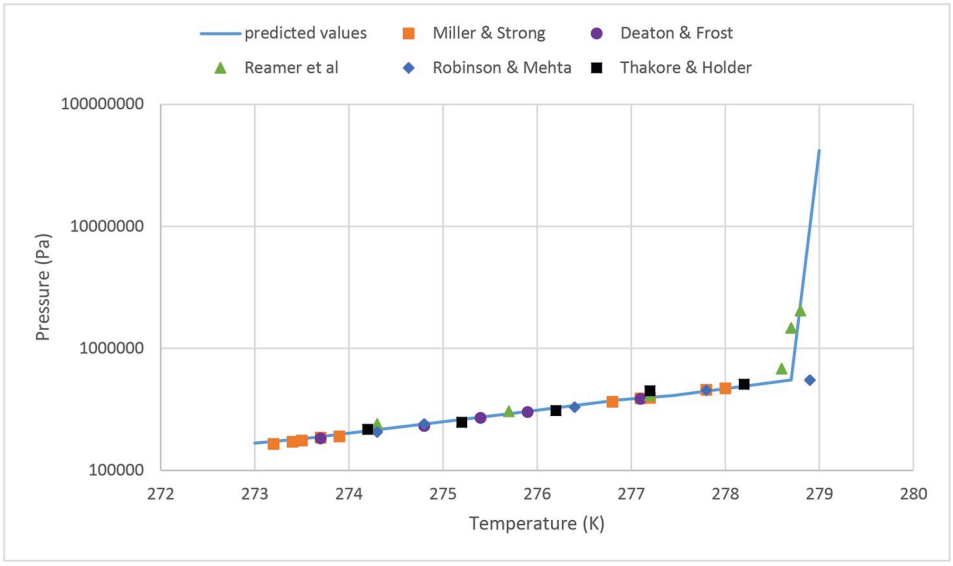

Fig. 3. Propane Hydrates pressure vs temperature.

laws for updating the connection weights are given by the following relationships (Haykin, 2009):

$$W_l = W_l + \eta\delta^k O_l^k \quad l = 1, ...L \tag{13}$$

$$W_{lj} = W_{lj} + \eta\delta^k W_l O_l^k (1 - O_l^k) x_j^k \qquad j = 1, \ n \ et \ l = 1, L \tag{14}$$

with:

$$\delta^k = (y^k - O^k) O^k (1 - O^k) \tag{15}$$

and:

W_l: Connection weight of the output layer
η: learning step
O_l^k: Output of cell l, belongs to the hidden layer and calculated for Example k

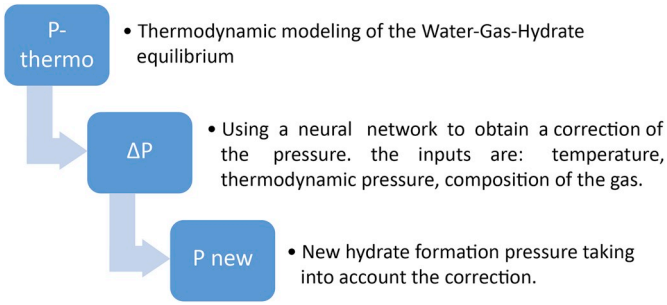

Fig. 4. Steps for calculating hydrate formation conditions using the thermodynamic modeling/neural networks combination.

Table 2
Average relative error obtained for some gases ([a] [Berecz, E. et al., 1983], [b] Rouher, O. S. et al., 1969, [c] Selleck, F.T. et al., 1952, [d] Holder, E. D. et al., 1982, [e] John, V. T. et al., 1985). * Mixture containing: N_2 0.42/CO_2 0.38/CH_4 45.59/C_2H_6 49.02/C_3H_8 4.53/i-C_4H_{10} 0.04/n-C_4H_{10} 0.02., ** Natural gas from În-Salah gas field: N_2 0.39/CO_2 3.64/CH_4 94.41/C_2H_6 1.42/C_3H_8 0.12/i-C_4H_{10} 0.01/n-C_4H_{10} 0.01., *** Natural gas from Hassi Messaoud/South oil field: N_2 2.3/CO_2 1.16/CH_4 51.63/C_2H_6 23.36/C_3H_8 15.61/i-C_4H_{10} 1.32/n-C_4H_{10} 3.71/C_5^+ 0.91.).

Gas	Temperature range (K)	Structure	Number of points	Source	ARE (%)	ARE (%)
CH_4	273–293.3	I	11	Villard [a]	2.8685	2.765
	273–286.6	I	4	Robert et al. [a]	2.59165	
	290.2–306.2	I	6	Marshall et al. [a]	6.99525	
	273.6–285.8	I	12	Deton and Frost [a]	0.35184	
	295.4–285.7	I	2	Kobayashi and Katz [a]	3.60079	
C_2H_6	273.6–28.9	I	6	Deaton and Frost (1) [a]	1.72188	
	274.7–286.4	I	15	Deaton and Frost (2) [a]	1.1708	
	273.25–287.9	I	11	Robert et al. [a]	4.58842	
C_3H_8	273.55–276.89	II	5	Deaton and Frost (1) [a]	2.4436	
	273.55–276.89	II	5	Deaton and Frost (2) [a]	2.4266	
	273.22–276.78	II	6	Frost and Deaton[a]	7.9574	
	273.05–277.95	II	15	Miller and Strong[a]	1.5887	
	274.12–277.7	II	4	Robinson and Mehta[a]	2.1804	
i-C_4H_{10}	273.18–275.05	II	24	Rouher and Barduhn [b]	4.8959	
N_2	273–284.5	I	18	Van Cleef and Diepen[a]	1.1172	
CO_2	277.05–282.89	I	5	Unruh and Katz [a]	2.8565	
	273.77–281.9	I	6	Robinson and Mehta[a]	1.3715	
H_2S	277.594–302.65	I	12	Selleck and sage [c]	1.9606	
C_2H_6 + C_3H_8	273.1–279.6	I/II	50	Holder and Hand [d]	2.6231	2.695
CO_2 + C_3H_8	273.93–281.82	II	9	Robinson and Mehta[e]	2.4588	
CH_4 + C_2H_6 + C_3H_8	279.76–284.98	II	9	Holder and Hand [d]	3.3330	
Mixture 1 (*)	275.977–292.24	II	13	Hysys	9.2237	9.2237
Mixture 2 (**)	275.413–282.418	II	8	Hysys	2.1937	2.1937
Mixture 3 (***)	273.729–293.26	II	8	Hysys	14.730	14.730

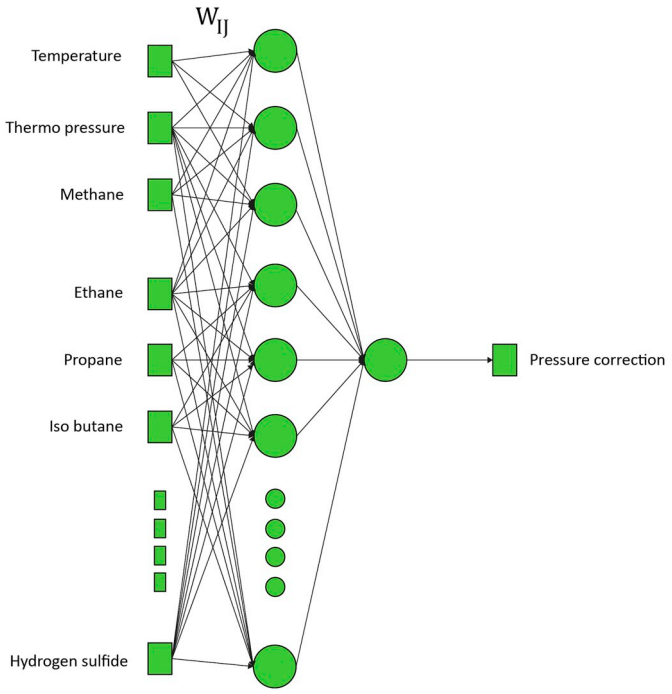

Fig. 5. Neural network architecture developed to correct pressure deviation.

Table 3
Temperature and components concentration ranges.

Parameter	Minimum	Maximum
Temperature (K)	273	318
Methane, Ethane, Propane, I-Butane (mol %)	0	100
N-Butane (mol %)	0	20
N_2 (mol %)	0	100
CO_2 (mol %)	0	100
H_2S (mol %)	0	100
C5+ (mol %)	0	5

Table 4
Characteristics and learning parameters of each neural network.

Network	Hidden neurons	β	λ	ϕ	K
1	8	0.5	0.70	0.270	0.043
2	24	0.6	0.80	0.303	0.004
3	21	0.6	0.70	0.403	0.040
4	23	0.7	0.75	0.310	0.041
5	23	0.7	0.78	0.340	0.040
6	20	0.5	0.70	0.270	0.043
7	22	0.5	0.63	0.309	0.046
8	23	0.5	0.68	0.305	0.055

W_{ij}: Connection weight of the hidden layer
O^k: Network output calculated for example k
$(x^k,\ y^k)$: Vector Inputs/Output of the example k
N and L: Number of cells in the input layer and the hidden layer respectively.

In order to accelerate the learning phase, to improve convergence, and to escape from local minima, the delta-bar-delta method was used with a B moment term.

According to this method, an individual learning rate is used for each weight that will be modified during the learning phase.

$$\eta^k = \eta^{k-1} + \Delta\eta^k \tag{16}$$

With:

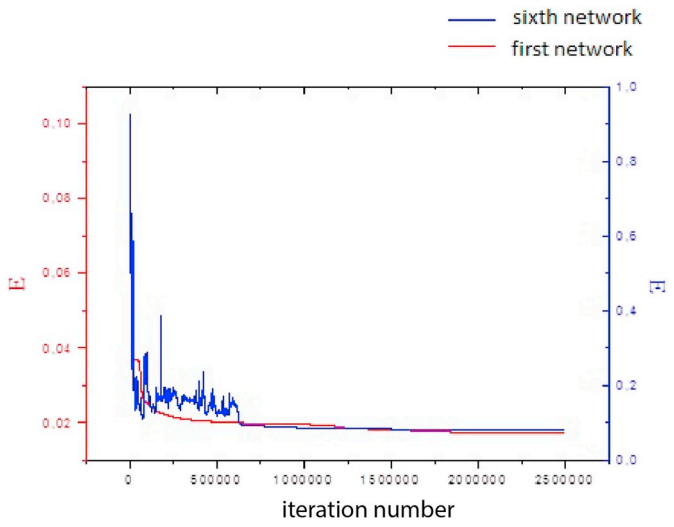

Fig. 6. Variation of E with respect to the number of iterations.

Table 5
Relative error obtained in the Learning Base.

Network	Number of points in the learning base	E (%)
1	70	2.762
2	740	2.646
3	826	2.441
4	963	2.935
5	961	3.155
6	774	3.534
7	708	3.181
8	1981	4.298

$$\Delta\eta^k = \begin{cases} K & if\ \bar{\delta}_{ij}(k-1)\cdot\delta_{ij}(k) > 0 \\ -\phi\eta_{ij}(k) & if\ \bar{\delta}_{ij}(k-1)\cdot\delta_{ij}(k) > 0 \\ 0 & Otherwise \end{cases} \tag{17}$$

and

$$\begin{cases} K > 0 \\ 0 < \phi < 1 \\ \delta_{ij}(k) = \frac{\partial E}{\partial w_{ij}}(k)\ and\ \bar{\delta}_{ij}(k) = (1-\lambda)\Delta\delta_{ij}(k) + \lambda\bar{\delta}_{ij}(k-1) \end{cases} \tag{18}$$

Better results are obtained when using in conjunction with delta-bar-delta a moment term.

$$\Delta w_{ij} = -\eta_{li}{}^k \frac{\partial E}{\partial w_{ij}}(k) + \beta\cdot\Delta w_{ij}(k-1) \tag{19}$$

4.2. Database

In order to build a database with Entry/Exit points we proceed as follows:

➢ Aspen Hysys simulator is used to calculate the hydrate formation pressure of a gas mixture at a fixed temperature. The models used in Hysys to predict hydrate formation conditions are based on fundamental thermodynamic principals (Van der waals –Platteeuw). There are two options: Ng & Robinson model (assumes that aqueous phase components have negligible solubility in other phases) and CSM model (Uses distinct equations of state for both aqueous and hydrocarbon phases). The latter is used in this work since it is the one recommended when components are partitioned between the aqueous and liquid hydrocarbon phases.

Table 6
Results of error analysis for thermodynamic modeling and for the combination with ANN in comparison with validation data.

Network	Components	Number of points	E (%) Thermodynamic modeling (Without ANN)	E (%) Using combination (With ANN)
1	$CH_4 + C_2H_6 + C_3H_8$	60	11.638	2.896
2	$CH_4 + C_2H_6 + C_3H_8 + N_2$	100	16.325	3.126
	$CH_4 + C_2H_6 + C_3H_8 + CO_2$	100	19.450	3.014
	$CH_4 + C_2H_6 + C_3H_8 + H_2S$	100	28.790	3.217
	$CH_4 + C_2H_6 + C_3H_8 + i\text{-}C_4H_{10}$	100	15.918	3.834
	$CH_4 + C_2H_6 + C_3H_8 + n\text{-}C_4H_{10}$	100	15.909	2.967
3	$CH_4 + C_2H_6 + C_3H_8 + CO_2 + H_2S$	60	29.970	3.748
	$CH_4 + C_2H_6 + C_3H_8 + CO_2 + i\text{-}C_4H_{10}$	60	23.955	3.897
	$CH_4 + C_2H_6 + C_3H_8 + CO_2 + n\text{-}C_4H_{10}$	60	13.763	2.782
	$CH_4 + C_2H_6 + C_3H_8 + i\text{-}C_4H_{10} + H_2S$	60	27.643	2.667
	$CH_4 + C_2H_6 + C_3H_8 + i\text{-}C_4H_{10} + n\text{-}C_4H_{10}$	60	22.023	3.783
	$CH_4 + C_2H_6 + C_3H_8 + N_2 + CO_2$	60	18.741	3.126
	$CH_4 + C_2H_6 + C_3H_8 + N_2 + H_2S$	60	28.300	3.283
	$CH_4 + C_2H_6 + C_3H_8 + N_2 + i\text{-}C_4H_{10}$	60	15.931	3.721
	$CH_4 + C_2H_6 + C_3H_8 + N_2 + n\text{-}C_4H_{10}$	60	14.187	2.327
	$CH_4 + C_2H_6 + C_3H_8 + n\text{-}C_4H_{10} + H_2S$	60	38.797	2.102
4	$CH_4 + C_2H_6 + C_3H_8 + CO_2 + i\text{-}C_4H_{10} + H_2S$	70	40.112	3.273
	$CH_4 + C_2H_6 + C_3H_8 + CO_2 + i\text{-}C_4H_{10} + n\text{-}C_4H_{10}$	70	25.402	2.651
	$CH_4 + C_2H_6 + C_3H_8 + CO_2 + n\text{-}C_4H_{10} + H_2S$	70	19.383	3.236
	$CH_4 + C_2H_6 + C_3H_8 + i\text{-}C_4H_{10} + n\text{-}C_4H_{10} + H_2S$	70	38.410	3.123
	$CH_4 + C_2H_6 + C_3H_8 + N_2 + CO_2 + H_2S$	70	31.274	1.789
	$CH_4 + C_2H_6 + C_3H_8 + N_2 + CO_2 + i\text{-}C_4H_{10}$	70	13.741	2.875
	$CH_4 + C_2H_6 + C_3H_8 + N_2 + CO_2 + n\text{-}C_4H_{10}$	70	31.141	3.138
	$CH_4 + C_2H_6 + C_3H_8 + N_2 + i\text{-}C_4H_{10} + H_2S$	70	14.688	3.247
	$CH_4 + C_2H_6 + C_3H_8 + N_2 + i\text{-}C_4H_{10} + n\text{-}C_4H_{10}$	70	28.271	2.917
	$CH_4 + C_2H_6 + C_3H_8 + N_2 + i\text{-}C_4H_{10} + H_2S$	70	15.298	3.674
5	$CH_4 + C_2H_6 + C_3H_8 + CO_2 + i\text{-}C_4H_{10} + n\text{-}C_4H_{10} + H_2S$	150	25.374	2.670
	$CH_4 + C_2H_6 + C_3H_8 + N_2 + CO_2 + i\text{-}C_4H_{10} + H_2S$	150	24.060	2.571
	$CH_4 + C_2H_6 + C_3H_8 + N_2 + CO_2 + i\text{-}C_4H_{10} + n\text{-}C_4H_{10}$	150	25.979	2.832
	$CH_4 + C_2H_6 + C_3H_8 + N_2 + CO_2 + n\text{-}C_4H_{10} + H_2S$	150	20.846	3.328
	$CH_4 + C_2H_6 + C_3H_8 + N_2 + i\text{-}C_4H_{10} + n\text{-}C_4H_{10} + H_2S$	150	32.436	2.897
6	$CH_4 + C_2H_6 + C_3H_8 + N_2 + CO_2 + i\text{-}C_4H_{10} + n\text{-}C_4H_{10} + H_2S$	600	27.093	2.671
7	$CH_4 + C_2H_6 + C_3H_8 + N_2 + CO_2 + i\text{-}C_4H_{10} + n\text{-}C_4H_{10} + C_5^+$	500	22.086	3.127
8	$CH_4 + C_2H_6 + C_3H_8 + N_2 + CO_2 + i\text{-}C_4H_{10} + n\text{-}C_4H_{10} + H_2S + C_5^+$	950	28.722	3.782

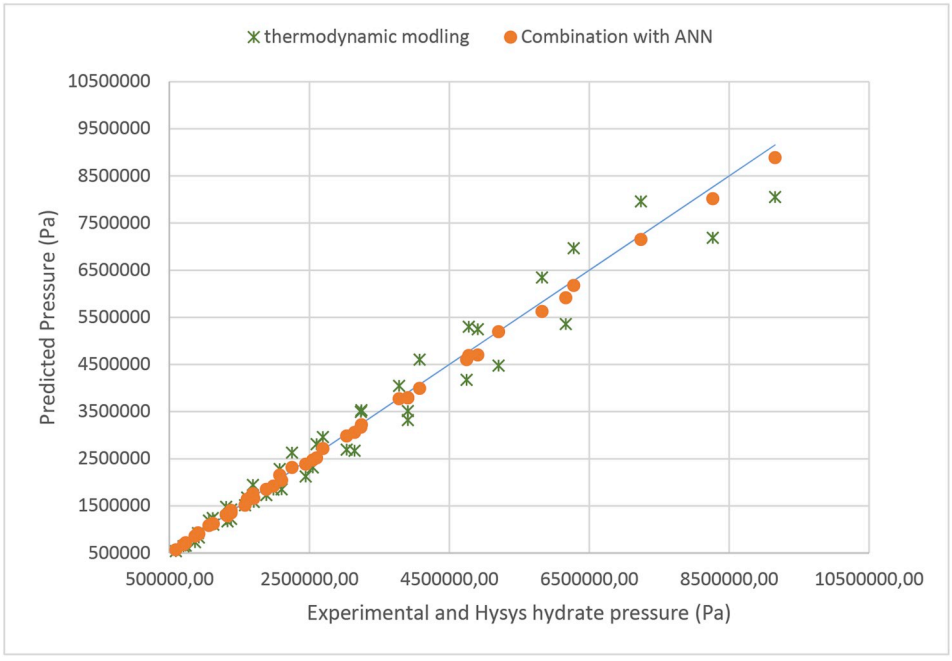

Fig. 7. Predicted pressures from thermodynamic modeling and the combination of thermodynamic with ANN vs database pressures values for different composition of a gas containing CH_4, C_2H_6 and C_3H_8. As shown in Table 6, the overall relative error obtained for 4660 points used for the validation phase, is of the order of 3.15%. This is a significant improvement on the overall relative error of around 23.75% that characterises the predictions of a pure thermodynamic model.

➢ In order to have a representative database, several gas compositions have been considered. For each composition, the temperature is varied and the hydrate formation pressure is calculated by Aspen Hysys. This phase is performed for 11403 points constituting the initial database. The range of variation of input parameters are shown in Table 3.

➢ The programming of the Van der Waals & Palttieuw model is used to recalculate the hydrate formation pressure for all points constituting the initial database. This program also calculates the difference between the pressure predicted by the thermodynamic model and that given by aspen Hysys (supposedly correct). The new database is composed of: The composition of the gas, the temperature, the

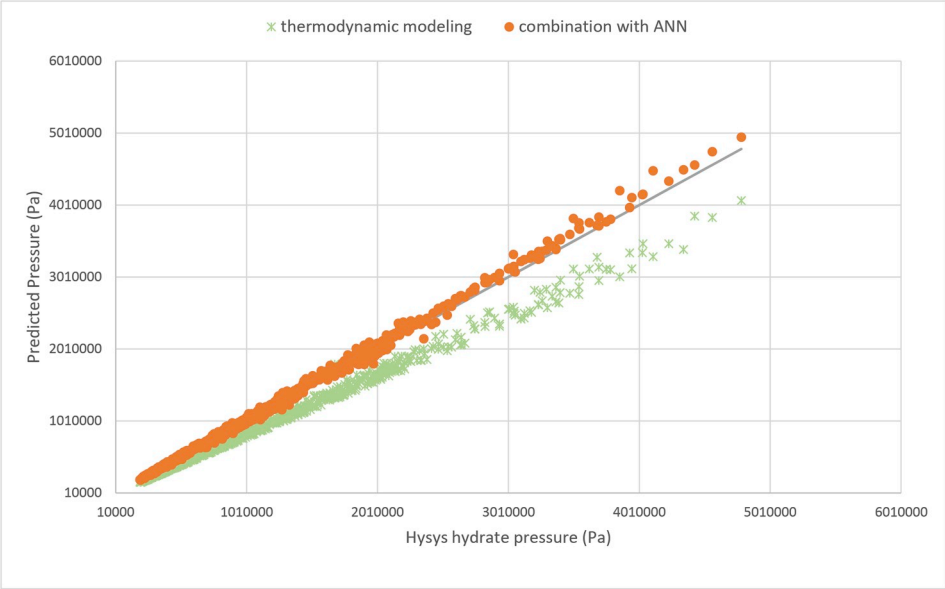

Fig. 8. Predicted pressures from thermodynamic modeling and the combination of thermodynamic with ANN vs database pressures values for different composition of a gas containing CH_4, C_2H_6, C_3H_8, iC_4H_{10}, nC_4H_{10}, C_5+, N_2, CO_2 and H_2S. (A detailed calculation of the deviation of the results from the database pressures is shown in Table 6.)

pressure calculated by applying the Van der Waals and Platteeuw model and the pressure difference obtained at the end of the calculation. The final database is simply called "database ".

Herein, we propose the use of eight neural networks instead of a single network. This involves subdividing the database into eight sub-databases. The proposed subdivision is based on the number of constituents present in the gas. The first network is called when the prediction is for a gas containing three elements (CH4, C2H6, C3H8), the second network is for a gas containing four elements (in addition to the three previous elements, the gas may contain CO_2 or N_2 or iC_4H_{10} or nC_4H_{10}) and so on.

We use a simple model to build the eight networks which have classical multilayer perceptron architecture with sigmoidal activation functions for the hidden neurons and the output neuron. We perform neural network training by applying gradient descent that minimizes the quadratic error, E, on the learning set. The learning phase continues until the error stabilizes at an almost fixed value. The number of neurons in the hidden layer and the adjustment parameters are determined by trial and error procedure until the error on the database designated for learning is the smallest possible. Table 4 shows the number of neurons in the hidden layer and the values of the adjustment parameters obtained at the end of this step for the eight neural networks. The symbols β, λ, ϕ, and K denote the appropriate adjustment parameters for the delta-bar-delta method.

The evolution of E during the learning phase is shown in Fig. 6. The latter illustrates the results obtained for the first and the sixth networks. The learning of all the networks is carried out until the error reaches a stable value. The values of the relative error obtained at the end of the learning phase of these networks are presented in Table 5.

4.3. Performance calculation

The database built at the beginning is divided into two parts. The first part is used for the learning phase in order to determine the values of the connection weights. The second part is deployed for validating the developed ANN model.

The comparison between the pressures predicted by thermodynamic modeling and the combination of thermodynamic modeling with the neuron network is illustrated in Fig. 7 (The first network) and 8 (The eighth network).

Fig. 7 shows the deviation of the predicted pressure using the first network for different composition of gases containing CH_4, C_2H_6 and C_3H_8, while Fig. 8 shows the predicted pressure using the eighth network for different composition of gases containing CH_4, C_2H_6, C_3H_8, iC_4H_{10}, nC_4H_{10}, C_5+, N_2, CO_2 and H_2S. In both figures, the combination significantly improves the prediction of the hydrate formation pressure.

The thermodynamic modeling of the hydrate formation conditions of a multi-component gas requires the use of reliable mixing rules and this still requires the adjustment of several parameters. This often makes the numerical solution slow and leads to convergence problems. This problem can be completely avoided by a reliable and fast tool ANN. The addition of a corrective term, developed using ANN, allows not only to have efficient results for a very wide range of temperature and composition (Table 3), but also to bypass all the complex problems emerging from the numerical resolution of equations presenting complex mixing rules.

5. Conclusion

Thermodynamic modeling of gas-hydrate-water equilibrium gives very satisfactory results for pure gases and binary mixtures. However, a significant deviation is noticed when it is applied for gas mixtures. A two-legged approach is developed to predict pressure hydrates formation for gas mixture systems. The approach combines thermodynamics modeling based on Van der Waals-Platteeuw model and deep learning using MLP ANN technique. The latter is used to approximate a pressure corrective term added to the thermodynamics predictions. The neurons networks are trained using the backpropagation algorithm fed with 4660 data points. The approach is able to reduce the overall relative error on the hydrate formation pressure of gas mixture systems to 3.15% down from 23%, which is the overall relative error when only a thermodynamic model is used. The results show that the learning phase of the neural networks is reached correctly and the approach can cover wide ranges of temperature and composition while avoiding problems associated with the use of complex mixing rules. The proposed approach presents a simple, fast, and yet accurate tool for improving the predictions of gas hydrates formation that are based on a thermodynamic model.

Appendix A. Supplementary data

Supplementary data to this article can be found online at https://

doi.org/10.1016/j.petrol.2019.106270.

References

Babakhani, S.M., Bahmani, M., Shariati, J., Badr, K., Balouchi, Y., 2015. Comparing the capability of artificial neural network (ANN) and CSMHYD program for predicting of hydrate formation pressure in binary mixtures. J. Pet. Sci. Eng. 136, 78–87.

Ballard, A.L., 2002. A Non-ideal Hydrate Solid Solution Model for Multi-phase Equilibria Program. PhD Thesis. Colorado school of mines, Colorado, USA.

Barkan, E.S., Sheinin, D.A., 1993. A general technique for the calculation of formation conditions of natural gas hydrates. J. Fluid Phase Equilib. 86, 111–136.

Berecz, E., Bella-achs, M., 1983. Gas Hydrates, Elsevier Edition, 1983.

Chapoy, A., Mohammadi, A.H., Richon, D., 2007. Predicting the hydrate stability zones of natural gases using artificial neural networks. Oil Gas Sci. Technol. 62 (5), 701–706.

Chen, G., Guo, T.M., 1996. Thermodynamic modelling of hydrate formation based on new concepts. Fluid Phase Equilib. 151, 43–65.

Elgibaly, A.A., Elkamel, A., 1998. A new correlation for predicting hydrate formation conditions for various gas mixtures and inhibitors. Fluid Phase Equilib. 152, 23–42.

Fausett, L.V., 1993. Fundamentals of Neural Networks. Pearson Edition, London, UK.

Fouad, W.A., Berrouk, A.S., 2012. Predictions of H2S and CO2 solubilities in aqueous triethanolamine solutions using a simple model of Kent-Eisenberg type. Ind. Eng. Chem. 51 (18), 6591–6597.

Fouad, Fouad, W.A., Berrouk, A.S., 2013. Phase Behavior of sour gas systems using classical and statistical thermodynamics equations of states. Fluid Phase Equilib. 356, 136–145.

Gbaruko, B.C., Igwe, J.C., Gbaruko, P.N., 2007. Gas hydrates and clathrates: flow assurance, environmental and economic perspectives and the Nigerian liquified natural gas project. J. Pet. Sci. Eng. 56 (1), 192–198.

Ghavipour, M., Chitsazan, M., Najibi, S.H., Ghidary, S.S., 2013. Experimental study of natural gas hydrates and a novel use of neural network to predict hydrate formation conditions. Chem. Eng. Res. Des. 91 (2), 264–273.

Gudmundsson, J.S., Børrehaug, A., 1996. In: Frozen Hydrate for Transport of Natural Gas, 2 International Conference on Natural Gas Hydrate, Toulouse, France.

Hamidreza, Y., Ali Kariman, M., Mohammad, M.G., 2014. Practical use of statistical learning theory for modeling freezing point depression of electrolyte solutions: LSSVM model. J. Nat. Gas Sci. Eng. 20, 414–421.

Hamidreza, Y., Mohammad, M.G., 2017. Modeling of gas hydrate phase equilibria: Extremely randomized trees and LSSVM approaches. J. Mol. Liq. 243, 533–541.

Hamidreza, Y., Mohammad, M.G., Amir, H.M., 2018. Determination of the gas hydrate formation limits to isenthalpic Joule-Thomson expansions. Chem. Eng. Res. Des. 132, 208–214.

Haykin, S., 2009. Neural Networks and Learning Machines, third ed. Pearson Edition, London, UK.

Helei, L., Christine, C., Patoon, T., Raphael, I., 2019. Analysis of CO2 equilibrium solubility of seven tertiary amine solvents using thermodynamic and ANN models. Fuel 249, 61–72.

Holder, G.D., Hand, J.H., 1982. Multiple-phase equilibria in hydrates from methane, ethane, propane and water mixtures. AIChE J. 28 (3), 440–447.

Holder, G.D., Zetts, S.P., Pradhan, N., 1988. Phase behavior in systems containing clathrate hydrates. Rev. Chem. Eng. 5 (1–4), 1–70.

Jassim, E.I., Abdi, M.A., Muzychka, Y., 2008. A CFD-based model to locate flow-restriction induced hydrate deposition in pipelines Offshore Technology. In: Conference. 2008. Offshore Technology Conference.

John, V.T., Papadopoulos, K.D., Holder, G.D., 1985. A generalized model for predicting equilibrium conditions for gas hydrates. AIChE J. 31 (2), 252–259.

Klauda, J.B., Snadler, S.I., 2003. Phase Behaviour of Clathrate Hydrates: a model for single end multiple gas component hydrates. Chem. Eng. Sci. 58, 27–41.

Ksabov, N., 1998. Foundations of Neural Networks, Fuzzy Systems, and Knowledge Engineering. Cambridge University Press, London, UK.

Lachet, V., Béhar, E., 2000. Industrial perspective on Natural gas hydrates. Oil Gas Sci. 55 (6), 611–616.

Lederhos, J., 1996. Effective kinetic inhibitors for natural gas hydrates. Chem. Eng. Sci. 51 (8), 1221–1229.

Mohammadi, A.H., Richon, D., 2010a. Hydrate phase equilibria for hydrogen + water and hydrogen + tetrahydrofuran + water systems: predictions of dissociation conditions using an artificial neural network algorithm. Chem. Eng. Sci. 65, 3352–3355.

Mohammadi, A.H., Richon, D., 2010b. Use of an artificial neural network algorithm to determine pressure-temperature phase diagrams of tert-butylamine + methane and tert-butylamine + hydrogen binary hydrates. Ind. Eng. Chem. Res. 45, 10141–10143.

Mohammadi, A.H., Martinez-lopez, D.F., 2010. Determining phase diagrams of tetrahydrofuran + methane, carbon dioxide or nitrogen clathrate hydrates using an artificial neural network algorithm. Chem. Eng. Sci. 65 (22), 6059–6063.

Mohammadi, A.H., Belandria, V., Richon, D., 2010. Use of an artificial neural network algorithm to predict hydrate dissociation conditions for hydrogen + water and hydrogen + tetra-n-butyl ammonium bromide + water systems. Chem. Eng. Sci. 65 (14), 4302–4305.

Mooijer–van den Heuvel, M.M., 2004. Phase Behaviour and Structural Aspects of Ternary Clathrate Hydrate System. PhD Thesis. Technische universiteit delft, Holland.

Moradi, M.R., Nazari, K., Alavi, S., Mohaddesi, M., 2013. Prediction of equilibrium conditions for hydrate formation in binary gaseous system using artificial neural networks. Energy Technol. 1, 171–176.

Nezhad, B.Z., Aminian, A., 2012. Accurate prediction of sour gas hydrate equilibrium dissociation conditions by using an adaptive neuro fuzzy inference system. Energy Convers. Manag. 57, 143–147.

Rouher, O.S., Barduhn, A.J., 1969. Hydrates of iso-and normal butane and their mixtures. Desalination 6, 57–73.

Selleck, F.T., Carmichael, L.T., Sage, B.H., 1952. Phase behaviour in the hydrogen sulfide-water system. Ind. Eng. Chem. 44 (9), 2219–2226.

Sloan, D.E., 1998. Clathrate Hydrates of Natural Gases, second ed. Marcel Dekker Inc.

Sloan, D.E., 1990. Natural gas hydrate phase equilibria and kinetics: understanding the stat of the art. Revue d'IFP 45 (2), 245–266.